

State-insensitive dichromatic optical-dipole trap for rubidium atoms: calculation and the dichromatic laser's realization

Junmin Wang¹, Shanlong Guo, Yulong Ge, Yongjie Cheng, Baodong Yang and Jun He

State Key Laboratory of Quantum Optics and Quantum Optics Devices (Shanxi University), and Institute of Opto-Electronics, Shanxi University, No. 92 Wu Cheng Road, Tai Yuan 030006, Shan Xi Province, People's Republic of China

E-mail: wjjmm@sxu.edu.cn

Received 13 November 2013, revised 12 March 2014

Accepted for publication 25 March 2014

Published 15 April 2014

Abstract

Magic wavelength optical-dipole trap (ODT) allows confinement of neutral atoms and cancellation of the position-dependent spatially inhomogeneous differential light shift for a desired atomic transition. The light shift of the ^{87}Rb $5P_{3/2}$ state can be expediently tailored to be equal to that of the ^{87}Rb $5S_{1/2}$ state by employing dichromatic ($\lambda_1 + \lambda_2$ (here $\lambda_2 = 2\lambda_1 \sim 1.5 \mu\text{m}$)) linearly polarized ODT lasers. In our calculation, two sets of state-insensitive dichromatic (784.3 + 1568.6 nm and 806.4 + 1612.8 nm) are obtained for the ^{87}Rb $5S_{1/2}$ ($F = 2$) – $5P_{3/2}$ ($F' = 3$) transition. Further, 784.3 + 1568.6 nm dichromatic laser system with a moderate output power has been realized experimentally by marrying efficient second-harmonic generation using a PPMgO:LN bulk crystal with a fibre-amplified 1.5 μm telecom laser.

Keywords: magic wavelength, dichromatic optical-dipole trap, 1.5 μm telecom laser, second-harmonic generation, PPMgO:LN crystal

(Some figures may appear in colour only in the online journal)

1. Introduction

Optical-dipole traps (ODTs) [1, 2] become important tools for trapping atoms with a low scattering rate [3–5]. The essence of an ODT is the potential due to the dipole interaction between the light-induced dipole moment of atoms and the laser intensity gradient. Generally, atomic states have different polarizabilities when interacting with certain wavelength and polarization laser beams, and thus will experience different light shifts when atoms are trapped in an ODT. So the desired atomic transition exhibits the position-dependent spatially inhomogeneous differential light shift compared to the case of undisturbed transition, and this will cause inhomogeneous dephasing, decreasing the coherence time of the quantum-state superposition in the process of coherent manipulation, especially for an ensemble of many atoms with finite temperature in an ODT [6, 7]. This presents challenges

for some applications, such as optical clock [8], quantum engineering, quantum metrology and quantum computing [9]. Fortunately, a magic wavelength (MW) ODT [8–12] working at a specific wavelength and polarization can not only trap atoms, but can also make the two states of the desired atomic transition experience an exactly equal light shift, therefore, cancelling the differential light shift for the transition. The MW ODT was proposed in 1999 for strontium (Sr) atoms [10] and later in 2003 for cesium (Cs) atoms [11, 12]. The implementation of MW ODT helps the optical clock [8, 9] with Sr atoms trapped in a standing-wave MW ODT to achieve a much lower uncertainty, and the quantum manipulation [9, 11] of the Cs atom trapped in a cavity-enhanced standing-wave MW ODT. Arora *et al* [13] calculated the monochromatic MWs for the nP – nS transitions in alkali metal atoms using the relativistic coupled-cluster method. Zhou *et al* [14] calculated the monochromatic MWs for terahertz-clock transitions of alkali-earth metal atoms. Phoonthong *et al* [15] experimentally implemented

¹ Author to whom any correspondence should be addressed.

and characterized the monochromatic MW ODT of Cs atoms. Arora *et al* [16] also focused on the calculations of the monochromatic MWs for the 5S–5P transition of Rb atoms, but many of the calculated values are not convenient for practical implementation. Lundblad *et al* [17] experimentally and Dereviako *et al* [18] theoretically discussed the possibility of the monochromatic MW with the assistance of an appropriate magnetic field for the clock transition of the alkali metal atoms. Following the experimental work on light-shift engineering with an auxiliary laser in an ODT carried out by Griffin *et al* [19], Arora and Sahoo [20] theoretically discussed a schematic of state-insensitive dichromatic optical trapping.

In this paper, we investigate a state-insensitive dichromatic ODT for ^{87}Rb atoms, which can cancel the differential light shift of the D_2 transition. We calculated and analysed the light shift of the ^{87}Rb $5S_{1/2}$ ($F = 2$) – $5P_{3/2}$ ($F' = 3$) transition in the case of a dichromatic ODT ($\lambda_1 + \lambda_2$ (here $\lambda_2 = 2\lambda_1 \sim 1.5 \mu\text{m}$)), and found the two sets of dichromatic MW (784.3 + 1568.6 nm and 806.4 + 1612.8 nm) for this transition. A distinct characteristic of the theoretical method is that we take the hyperfine structure and the corresponding Zeeman sub-levels into account in our calculation. This is convenient for direct comparison with experiments in which the Rb atoms in this ODT are prepared on the desired Zeeman states of a certain hyperfine level using optical pumping. In experiment, 784.3 + 1568.6 nm dichromatic ODT laser system with a moderate output power has been realized by marrying the second-harmonic generation (SHG), using a quasi-phase-matching (QPM) PPMgO:LN bulk crystal, with a fibre-amplified 1.5 μm telecom laser, which will be used in the confinement of ^{87}Rb atoms.

2. Calculation method for light shift

The light shift of the atomic state arises from the dipole interaction between the induced atomic dipole moment $\vec{d}(r)$ and the position-dependent light field $\vec{E}(r)$. According to the oscillator model, the light shift $U_{\text{dip}}(r)$ can be given as [1]

$$U_{\text{dip}}(r) = -\frac{1}{2}(\vec{d}(r) \cdot \vec{E}(r)) = -\frac{1}{2\epsilon_0 c} \text{Re}[\alpha(\omega)]I(r). \quad (1)$$

Here $\vec{d}(r) = \alpha(\omega)\vec{E}(r)$, $\alpha(\omega)$ is the polarizability that depends on the light frequency ω and atomic state, $\text{Re}[\alpha(\omega)]$ is the real part of $\alpha(\omega)$, c is the light speed in vacuum, ϵ_0 is the vacuum dielectric constant, and $I(r) = 2\epsilon_0 c |\vec{E}(r)|^2$ is the light intensity. The angular brackets denote the time average over the rapid oscillating terms with the light frequency. In the case of the red detuned laser, $U_{\text{dip}}(r)$ for the atomic ground state is negative and has a maximum light shift at the maximum-intensity points (for example, the focal point of a focused TEM₀₀-mode Gaussian laser beam [2, 4, 5, 12, 15] or the antinodes of a standing-wave laser field [8, 11]), thus it can attract atoms to the points. In contrast, in the case of the blue detuned laser, $U_{\text{dip}}(r)$ for the atomic ground state is positive, and it repulses atoms to the point with the minimum intensity (the dark region of a hollow laser beam or a bottle laser beam [1, 3]).

In order to determine the light shift $U_{\text{dip}}(r)$ with the given $\vec{E}(r)$ of an ODT, the main task is to calculate the polarizability

$\alpha(\omega)$. For the atomic state $|IJFM\rangle$ with a nuclear spin of I , an angular momentum of J , a total angular momentum of F , and a magnetic quantum number of M , if we consider the case of a far-off-resonance ODT, in which the light field drives atoms well below saturation and the detuning also far exceeds all hyperfine splittings, we can neglect the hyperfine splittings. So we can assume that all the dipole-allowed transitions from the $|IJFM\rangle$ state to the $|IJ'F'M'\rangle$ states with all possible F' and M' but with the same J' have approximately the same angular transition frequency $\omega_{JJ'}$. $\alpha(\omega)$ of the $|IJFM\rangle$ state can be calculated by summing up the contributions of many dipole-allowed transitions connected with this state:

$$\alpha(\omega) = 6\pi c^3 \epsilon_0 \sum_{J', F', M'} \frac{1}{\omega_{JJ'}^2 (\omega_{JJ'}^2 - \omega^2)} |\langle IJ'F'M' | \hat{d} | IJFM \rangle|^2 \times \frac{\omega_{JJ'}^3}{3\pi \epsilon_0 \hbar c^3}. \quad (2)$$

Here ω is the angular frequency of the ODT laser, \hat{d} is the dipole operator, and $\langle IJ'F'M' | \hat{d} | IJFM \rangle$ is the dipole matrix element. The next task is the reduction of the dipole matrix element. The term $|\langle IJ'F'M' | \hat{d} | IJFM \rangle|^2$ can be expressed as follows [21]:

$$|\langle IJ'F'M' | \hat{d} | IJFM \rangle|^2 = (2F + 1) | \langle J' || \hat{d} || J \rangle |^2 \times \left| \begin{Bmatrix} J & J' & 1 \\ F' & F & I \end{Bmatrix} \right|^2 |c_{F,M}^{F',M'}|^2. \quad (3)$$

Here the part in curly brackets is the Wigner 6-j symbol (computed using the Mathematica function ‘SixJSymbol’), and the shorthand notation $c_{F,M}^{F',M'}$ is the Clebsch–Gordan coefficients, and it is explicitly given as follows [21]:

$$c_{F,M}^{F',M'} = \langle FM | p | F'M' \rangle = (-1)^{M+F-1} \sqrt{2F'+1} \times \begin{pmatrix} F & 1 & F' \\ M & p & -M' \end{pmatrix}. \quad (4)$$

Here the part in round brackets is the Wigner 3-j symbol (computed using the Mathematica function ‘ThreeJSymbol’), and p stands for linear polarization ($p = 0$) and σ^\pm circular polarizations ($p = \pm 1$), the selection rule is $M' = M + p$. For simplicity, here we only consider a linearly-polarized ODT laser beam. We choose the following normalization for the reduced matrix element, expressed in terms of the Einstein coefficient $A_{J' \rightarrow J}$ of the fine state J' in the case of one decay channel $J' \rightarrow J$, and we also regard that all dipole-allowed transitions from the $|IJ'F'M'\rangle$ states with all possible F' and M' but with the same J' to the $|IJFM\rangle$ state have the same $A_{J' \rightarrow J}$ coefficient [21]:

$$| \langle J' || \hat{d} || J \rangle |^2 = A_{J' \rightarrow J} (2J' + 1) \frac{3\pi \epsilon_0 \hbar c^3}{\omega_{JJ'}^3}. \quad (5)$$

Combining formulas (3), (4) and (5) with (2), if we know $\omega_{JJ'}$ and $A_{J' \rightarrow J}$, we can get $\alpha(\omega)$ of the $|IJFM\rangle$ state. In our calculation, the $A_{J' \rightarrow J}$ data and the angular transition frequency $\omega_{JJ'}$ data ($\omega_{JJ'} = 2\pi c / \lambda_{JJ'}$, $\lambda_{JJ'}$ is the vacuum wavelength) originate from [22]. Further we can calculate $U(r)$ for atomic ground and excited states for the given $\vec{E}(r)$. To check the validity of this method, we computed the monochromatic MW for the Cs $6S_{1/2}$ $|F = 4, M_F = +4\rangle - 6P_{3/2}$ $|F' = 5,$

$M_F = +5$) transition, and got the calculated value of 935.6 nm, which is consistent with the previous calculations [11, 12, 21] and experiments [11, 15]. This indicates the calculation method is valid even if we made some approximations. In addition, a characteristic of this method is that we take the hyperfine structure and the corresponding Zeeman sub-levels into consideration, and it is convenient for direct comparison with experiments in which the trapped atoms in this ODT are prepared on the desired Zeeman state of the hyperfine level.

3. State-insensitive dichromatic ODT scheme for ^{87}Rb atoms

We focused on the ^{87}Rb $5S_{1/2} |F = 2, M_F = +2\rangle$ (denoted by |1>) $-5P_{3/2} |F' = 3, M_F = +3\rangle$ (denoted by |2>) transition. The interest was motivated by the following story. Darquie *et al* [4] demonstrated a triggered single-photon source based on a single ^{87}Rb atom confined in a tightly-focused 810 nm microscopic ODT, in which the trapped atom was periodically excited by a series of laser π -pulses to drive the closed |1>-|2) transition. However, the ODT induced position-dependent differential light shift of the |1>-|2) transition, thus the atomic residual motion will partially smear out the indistinguishability of the single photons because it leads to different centre frequency. If one implements a MW ODT for the |1>-|2) transition, the above-mentioned issue may be solved.

Firstly we calculated the light shift of the |1) and |2) states in the case of a monochromatic ODT. The laser intensity is reasonably chosen at $\sim 5 \times 10^4 \text{ W cm}^{-2}$. Our calculation gives the monochromatic MWs of 625.3 and 789.9 nm for the ^{87}Rb |1>-|2) transition, which are similar to the previous calculation [11]. Around 625.3 and 789.9 nm, the polarizabilities of the |1) and |2) states are too small to form an ODT in practice (for convenient laser intensity $\leq 1 \times 10^5 \text{ W cm}^{-2}$). Also a high-power laser with these wavelengths is not convenient to implement.

Now let us discuss the state-insensitive dichromatic ODT scheme for ^{87}Rb atoms. The relevant fine energy levels are shown in figure 1 (not to scale). When an ODT is implemented with the dichromatic laser beams of wavelength λ_1 and $\lambda_2 = 2\lambda_1 \sim 1.5 \mu\text{m}$ with the same linear polarizations and equal intensity, the $5P_{3/2} - 4D_{3/2}$ and $5P_{3/2} - 4D_{5/2}$ transitions with wavelengths of 1529.3 and 1529.4 nm will dominate the light shift of the $5P_{3/2}$ state because the λ_2 laser is close to these transitions, while the $5S_{1/2} - 5P_{1/2}$ and $5S_{1/2} - 5P_{3/2}$ transitions will dominate the light shift of the $5S_{1/2}$ state because the λ_1 laser now is close to these transitions. The light shift of the ^{87}Rb $5S_{1/2}$ and $5P_{3/2}$ states may be tailored to be equal by selecting proper wavelength λ_1 , because the scalar polarizabilities of the $5S_{1/2}$ and $5P_{3/2}$ states have different wavelength-dependent behaviours and maybe have crossing. A commercial $1.5 \mu\text{m}$ telecom laser with a fibre amplifier can be employed to serve as the λ_2 laser, and the λ_1 laser can be achieved by frequency doubling of the $1.5 \mu\text{m}$ telecom laser [23]. Actually the Bouyer and Barrett groups [24–26] recently utilized a 1560 nm laser to form a monochromatic ODT to confine ^{87}Rb atoms for the light-shift tomography, atomic interferometer, and self-organization threshold scaling

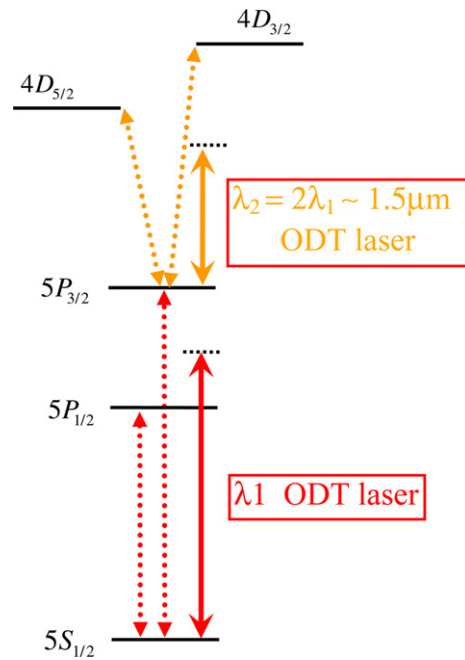


Figure 1. Relevant fine energy levels of ^{87}Rb atoms (not to scale). When an ODT is implemented with the dichromatic laser beams of wavelength λ_1 (the red solid line with arrows) and $\lambda_2 = 2\lambda_1 \sim 1.5 \mu\text{m}$ (the orange solid line with arrows), the transitions connected with the $5S_{1/2}$ state marked by the red dotted lines will dominate the light shift of the $5S_{1/2}$ state, and the transitions connected with the $5P_{3/2}$ state marked by the yellow dotted lines will dominate the light shift of the $5P_{3/2}$ state. The light shift of the $5S_{1/2}$ and $5P_{3/2}$ states may be tailored to be equal by selecting proper wavelength λ_1 , because the scalar polarizabilities of the $5S_{1/2}$ and $5P_{3/2}$ states have different wavelength-dependent behaviours and maybe have crossing.

for thermal atoms coupled to a cavity, respectively. For simplicity, we assume that λ_1 and $\lambda_2 = 2\lambda_1 \sim 1.5 \mu\text{m}$ laser beams have the same linear polarization and equal intensity (fixed at $3.6 \times 10^4 \text{ W cm}^{-2}$ reasonably). Taking the $nS_{1/2}$ states from $5S_{1/2}$ to $10S_{1/2}$, $nP_{1/2}$ states from $5P_{1/2}$ to $10P_{1/2}$, $nP_{3/2}$ states from $5P_{3/2}$ to $10P_{3/2}$, $nD_{3/2}$ states from $4D_{3/2}$ to $8D_{3/2}$, and $nD_{5/2}$ states from $4D_{5/2}$ to $8D_{5/2}$ into consideration, we performed calculation of the light shift of ^{87}Rb $5S_{1/2} |F = 2, M_F = \pm 2\rangle$ and $5P_{3/2} |F' = 3, M_F = \pm 3\rangle$ states, and the results are shown in figure 2.

The calculated light shifts of the $M_F = 0, \pm 1, \pm 2$ Zeeman sublevels of the $F = 2$ state are almost the same and are shown by the blue dashed line, while the light shift of the $M_F = \pm 3$ Zeeman sublevels of $F' = 3$ state are shown by the red solid line, and that of the $M_F = 0, \pm 1, \pm 2$ Zeeman sublevels are shown by the other three black solid lines. Two circles in figure 3 indicate the two sets of state-insensitive dichromatic wavelength combination (784.3 + 1568.6 nm and 806.4 + 1612.8 nm) for ^{87}Rb $5S_{1/2} |F = 2, M_F = \pm 2\rangle - 5P_{3/2} |F' = 3, M_F = \pm 3\rangle$ transitions.

We analysed the effect of variation in the laser wavelength (but the ratio is kept at $\lambda_2 = 2\lambda_1$) upon the light shift of ^{87}Rb |1) and |2) states. The data are given with λ_1 and λ_2 lasers at an equal intensity of $2.94 \times 10^4 \text{ W cm}^{-2}$ for $\lambda_1 = 784.3$ and $\lambda_2 = 1568.6$ nm lasers ($6.17 \times 10^4 \text{ W cm}^{-2}$ for 806.4 and 1612.8 nm lasers), which forms a dichromatic ODT with a

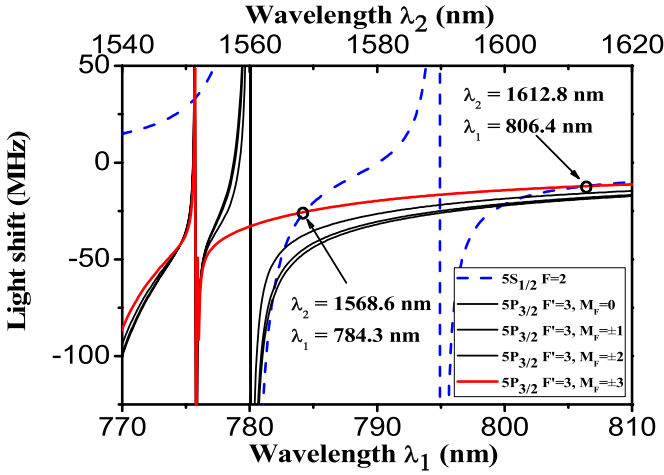


Figure 2. The calculated light shifts of the ^{87}Rb $5S_{1/2}$ ($F = 2$) state (the blue dashed line, the light shift for all the $M_F = 0, \pm 1, \pm 2$ Zeeman sublevels is almost the same) and the $5P_{3/2}$ ($F' = 3$) state (the red solid line for the $M_F = \pm 3$ Zeeman sublevels, the other three black solid lines for the $M_F = 0, \pm 1, \pm 2$ Zeeman sublevels) in the case of the dichromatic ODT with the same linearly polarized laser beams of wavelengths λ_1 and $\lambda_2 = 2\lambda_1 \sim 1.5 \mu\text{m}$. Intensities of the λ_1 and λ_2 lasers are equal and fixed to $3.6 \times 10^4 \text{ W cm}^{-2}$ reasonably. No transition line exists for $F = 2$ and $F' = 3$ states in the wavelength range from 1540 to 1620 nm. The zero-crossings correspond to 776 nm $5P_{3/2}-5D_{3/2}(5D_{5/2})$ transitions (two lines are too close to distinguish), 780.2 nm D_2 transition, and 794.9 nm D_1 transitions. Two circles indicate two sets of the state-insensitive dichromatic.

Table 1. Effect of variation in the dichromatic ODT laser's wavelength λ_1 and $\lambda_2 = 2\lambda_1 \sim 1.5 \mu\text{m}$ upon the light shift of ^{87}Rb $5S_{1/2}$ ($F = 2, M_F = +2$) ($|1\rangle$) and $5P_{3/2}$ ($F' = 3, M_F = +3$) ($|2\rangle$) states. The data are given with both lasers at the same intensity of $2.94 \times 10^4 \text{ W cm}^{-2}$ for the 784.3 + 1568.6 nm set ($6.17 \times 10^4 \text{ W cm}^{-2}$ for 806.4 + 1612.8 nm set), which forms a dichromatic ODT with a trap depth of $T_{\text{ODT}} = U/k_B \sim 1 \text{ mK}$.

λ_1 (nm)	$\Delta\lambda_1$ (nm)	$\lambda_2 = 2\lambda_1$ (nm)	T_{ODT} (mK) for state $ 1\rangle T_{\text{ODT}} = U/k_B$	T'_{ODT} (mK) for state $ 2\rangle T'_{\text{ODT}} = U'/k_B$	Potential difference $(U' - U)/U$
784.2	-0.1	1568.4	-1.0304	-1.0048	-2.5%
784.3	0.0	1568.6	-1.0000	-1.0006	+0.1%
784.4	+0.1	1568.8	-0.9689	-0.9945	+2.6%
806.3	-0.1	1612.6	-1.0066	-1.0035	-0.3%
806.4	0.0	1612.8	-1.0000	-1.0006	+0.1%
806.5	+0.1	1613.0	-0.9947	-0.9989	+0.4%

Table 2. Effect of variation in the intensity ratio between the λ_1 and $\lambda_2 = 2\lambda_1 \sim 1.5 \mu\text{m}$ lasers of the dichromatic ODT upon the light shift of ^{87}Rb $5S_{1/2}$ ($F = 2, M_F = +2$) ($|1\rangle$) and $5P_{3/2}$ ($F' = 3, M_F = +3$) ($|2\rangle$) states. The laser intensity is the same as in table 1.

λ_1 (nm)	$\lambda_2 = 2\lambda_1$ (nm)	I_2/I_1	T_{ODT} (mK) for state $ 1\rangle T_{\text{ODT}} = U/k_B$	T'_{ODT} (mK) for state $ 2\rangle T'_{\text{ODT}} = U'/k_B$	Potential difference $(U' - U)/U$
784.3	1568.6	0.90	-0.9973	-0.9023	-9.5%
		0.95	-0.9987	-0.9515	-4.7%
		0.99	-0.9997	-0.9908	-0.9%
		1.00	-1.0000	-1.0006	+0.1%
		1.01	-1.0003	-1.0105	+1.0%
		1.05	-1.0014	-1.0498	+4.8%
806.4	1612.8	1.10	-1.0027	-1.0990	+9.6%
		0.90	-0.9944	-0.8989	-9.6%
		0.95	-0.9972	-0.9497	-4.8%
		0.99	-0.9994	-0.9904	-0.9%
		1.00	-1.0000	-1.0006	+0.1%
		1.01	-1.0006	-1.0107	+1.0%
1.05	-1.0028	-1.0514	+4.9%		
1.10	-1.0056	-1.1023	+9.6%		

typical trap depth of $T_{\text{ODT}} = U/k_B \sim 1 \text{ mK}$ (k_B is the Boltzman constant). The results are given in table 1. The wavelength variations of $\pm 0.1 \text{ nm}$ only make a difference within $\pm 2.6\%$ for the 784.3 + 1568.6 nm case (within $\pm 0.4\%$ for the 806.4 + 1612.6 nm case) in the light shifts of $|1\rangle$ and $|2\rangle$ states. Actually the variation in the laser wavelength can be easily kept below $\pm 0.01 \text{ nm}$ in experiment, so the influence of wavelength variation can be neglected.

We also analysed the effect of variation in the intensity ratio between the dichromatic laser beams upon the light shift. The results are given in table 2, and the centre values of laser intensity are kept the same as in table 1. The relative fluctuations ($\pm 1\%$, $\pm 5\%$, and $\pm 10\%$) in the intensity ratio will not have a substantial effect (within $\pm 9.6\%$). Actually the variation in the intensity ratio can be maintained below $\pm 1\%$ in experiment, resulting in the light shift varying within $\pm 1.0\%$. From the above discussion on the effect of fluctuations in the wavelength and intensity ratio of the two lasers on light shifts, our proposed state-insensitive dichromatic ODT should be available in practice. The inhomogeneous dephasing mainly comes from the residual thermal motion of trapped atoms in the ODT with differential light shifts for the desired transition connected ground state with the excited state. Further cooling atoms with polarization gradient cooling phase can decrease the residual motion of trapped atoms, and now state-insensitive dichromatic ODT (or dichromatic MW ODT) can eliminate the differential light shifts.

4. The experimental realization of the state-insensitive dichromatic laser system

For implementing the state-insensitive dichromatic ODT, we proposed and have experimentally realized a 784.3 + 1568.6 nm dichromatic laser system based on SHG from a 1568.6 nm telecom laser to 784.3 nm by using a QPM PPMgO:LN bulk crystal. This dichromatic laser system is based on our previous work, in which 239 mW of the 780 nm laser beam was achieved via single-pass SHG with a 20 mm long type-I PPLN crystal (Deltronics Inc, the poling period $\Lambda = 18.8 \mu\text{m}$) with an Er-doped fibre amplifier (EDFA, Keopsys) boosted 1560 nm telecom laser [23]. To avoid the photo-refractive damage (PRD) we had to operate the PPLN crystal at a temperature $\sim 162^\circ\text{C}$ [23]. According to our estimation, if we tune the fundamental-wave laser to 1568.6 nm, the QPM temperature for SHG will be higher than 200°C , which is not convenient. So in our new setup we replaced the PPLN crystal with a 25 mm long type-I PPMgO:LN crystal (HC Photonics, the poling period $\Lambda = 19.48 \mu\text{m}$). The doping of MgO can efficiently avoid PRD, and also allows lower temperature operation. The typical QPM temperature is $\sim 126.7^\circ\text{C}$ for SHG of 1568.6 nm, and no PRD is observed.

The 784.3 + 1568.6 nm dichromatic laser system is schematically shown in figure 3. The EDFA boosts the 1568.6 nm seeded laser to ~ 4 W. A 25 mm long PPMgO:LN bulk crystal is housed in an oven, and the oven temperature can be stabilized at $126.70 \pm 0.01^\circ\text{C}$. The EDFA output laser beam is focused into the PPMgO:LN crystal and then collimated after passing through the crystal by using two lenses ($f = 50$ mm). We use a dichromatic mirror (DM) to separate 1568.6 and 784.3 nm laser beams. Then we can adjust the power of two laser beams to reach equal intensity by using half-wave plate ($\lambda/2$) and polarization beam splitter cube (PBS). Finally two laser beams are recombined by another DM. An achromatic doublet lens can be utilized to remove the colour aberration and focus these dichromatic travelling laser beams (not standing waves for the different periodicity between the 1568.6 and 784.3 nm laser) into an ultra-high-vacuum chamber to form the state-insensitive dichromatic

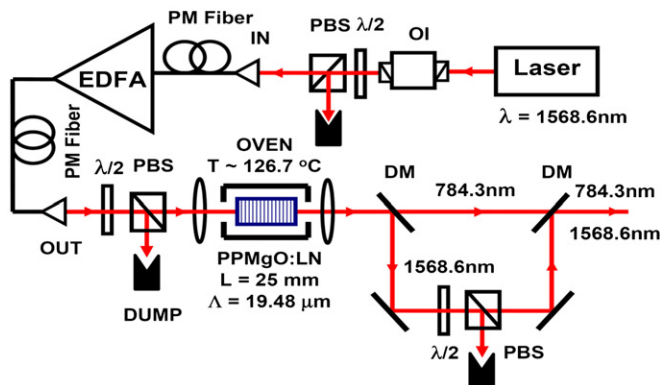


Figure 3. Schematic diagram of the 784.3 + 1568.6 nm dichromatic laser. OI: optical isolator; PBS: polarization beam splitter cube; PM fibre: polarization-maintained optical fibre; EDFA: Er-doped fibre amplifier; $\lambda/2$: half-wave plate; DM: dichromatic mirror.

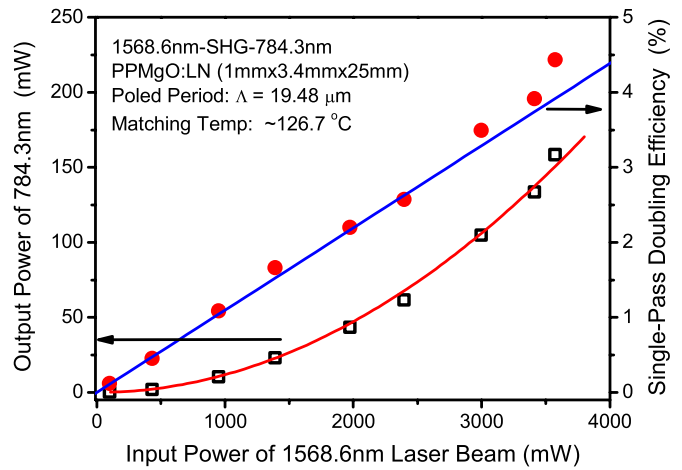


Figure 4. The 784.3 nm harmonic wave's output (black hollow squares) and the single-pass doubling efficiency (red dots) versus the 1568.6 nm fundamental wave's input power. The solid lines are fitting based on the SHG theoretical model.

ODT with $\sim 15 \mu\text{m}$ of the waist radius, where ^{87}Rb atoms are laser cooled and trapped. Here, the quantization axis of atoms can be set perpendicular to the propagation direction of the ODT lasers and parallel to their polarization axes.

The measured 784.3 nm laser's output and the corresponding single-pass doubling efficiency as a function of the 1568.6 nm input are plotted in figure 4. 158 mW of 784.3 nm output is achieved when the 1568.6 nm input is 3.6 W, corresponding to 4.4% of the doubling efficiency. Supposing a focused laser beam with $\sim 15 \mu\text{m}$ of the waist radius and ~ 100 mW of each laser's power, the trap depth of this dichromatic WM ODT will be $T_{\text{ODT}} = U/k_B \sim 1$ mK, which is deep enough to trap laser-cooled ^{87}Rb atoms. In principle, another set of the state-insensitive dichromatic (806.4 + 1612.8 nm) can also be implemented using the same technique.

For an ODT, heating and photon-scattering rates are important parameters especially when the wavelength of ODT optical fields is close to the atomic transition line. For our case, when the atoms are trapped in the dichromatic ODT, they are populated on the ground states $5S$ in the most time, so the photon-scattering rates are mainly from the contribution of the 784.3 nm (or 806.4 nm) laser beam, which are close to ^{87}Rb 's 780 nm transition line. In calculation, we ignore the contribution of the photon-scattering rate from the 1568.6 nm (or 1612.8 nm) laser beam. For the (784.3 + 1568.6 nm) state-insensitive ODT, we estimate that the photon-scattering rate is ~ 550 photons s^{-1} with the ~ 1 mK trap depth, and the corresponding heating rate is $\sim 2.8 \times 10^{-10} \mu\text{K s}^{-1}$. For the (806.4 + 1612.8 nm) state-insensitive ODT, it will give a lower photon-scattering rate ~ 100 photons s^{-1} with the same trap depth, and corresponding heating rate $\sim 5.0 \times 10^{-11} \mu\text{K s}^{-1}$.

5. Conclusion

In conclusion, we calculated and analysed the light shift of the ^{87}Rb $5S_{1/2} - 5P_{3/2}$ transition for a dichromatic linearly-polarized ODT ($\lambda_1 + \lambda_2$ (here $\lambda_2 = 2\lambda_1 \sim 1.5 \mu\text{m}$), and found that the state-insensitive dichromatic for the ^{87}Rb $5S_{1/2}$ $|F = 2$,

$M_F = +2\rangle - 5P_{3/2} |F' = 3, M_F = +3\rangle$ transition exists at (784.3 + 1568.6 nm) and (806.4 + 1612.8 nm) with equal intensity of the λ_1 and λ_2 laser beams. We also discussed the influence of wavelength fluctuation and intensity ratio of the two lasers near the theoretical values on dichromatic ODT. In addition, we realized (784.3 + 1568.6 nm) dichromatic laser system by marrying SHG using a PPMgO:LN bulk crystal with an EDFA-amplified 1.5 μm telecom laser in experiment. Our state-insensitive dichromatic ODT experiment is under way.

Based on the single ^{87}Rb atom trapped in this state-insensitive dichromatic ODT, it is possible to realize a triggered single-photon source with much more indistinguishable photons [27, 28], which are important issues for performing an ideal Hong–Ou–Mandel two-photon quantum interference [29, 29] and the quantum computation and quantum information processing with linear optics techniques [31, 32]. This state-insensitive dichromatic ODT scheme may be extended to other species and it may find more applications in the precision measurement of atomic transition frequency and the optical clock [8–10], the state-insensitive atomic quantum engineering [9, 11], the coherent manipulation of atomic internal state independent of the residual thermal motion.

Acknowledgments

This project is supported by the National Major Scientific Research Program of China (grant no 2012CB921601), the National Natural Science Foundation of China (grant nos 11274213, 61227902, 61205215, 11104172 and 61121064), the Shanxi Scholarship Council of China (grant no 2012-015), and Research Program for Science and Technology Star of Taiyuan, Shanxi, China (grant no 12024707).

References

- [1] Grimm R, Weidemüller M and Ovchinnikov Y B 2000 *Adv. At. Mol. Opt. Phys.* **42** 95
- [2] Miller J D, Cline R A and Heinzen D J 1993 *Phys. Rev. A* **47** 4567(R)
- [3] Li G, Zhang S, Isenhower L, Maller K and Saffman M 2012 *Opt. Lett.* **37** 851
- [4] Darquie B, Jones M P A, Dingjan J, Beugnon J, Bergamini S, Sortais Y, Messin G, Browaeys A and Grangier P 2005 *Science* **309** 454
- [5] He J, Yang B D, Zhang T C and Wang J M 2011 *Phys. Scr.* **84** 025302
- [6] Kuhr S, Alt W, Schrader D, Dotsenko I, Miroshnychenko Y, Rauschenbeutel A and Meschede D 2005 *Phys. Rev. A* **72** 023406
- [7] Jones M P A, Beugnon J, Gaëtan A, Zhang J, Messin G, Browaeys A and Grangier P 2007 *Phys. Rev. A* **75** 040301R
- [8] Takamoto M, Hong F-L, Higashi R and Katori H 2005 *Nature* **435** 321
- [9] Ye J, Kimble H J and Katori H 2008 *Science* **320** 1734
- [10] Katori H, Ido T and Kuwata-Gonokami M 1999 *J. Phys. Soc. Japan* **68** 2479
- [11] McKeever J, Buck J R., Boozer A D, Kuzmich A, Nagerl H-C, Stamper-Kurn D M and Kimble H J 2003 *Phys. Rev. Lett.* **90** 133602
- [12] Kim J Y, Lee J S, Han J H and Cho D 2003 *J. Korean Phys. Soc.* **42** 483
- [13] Arora B, Safronova M S and Clark C W 2007 *Phys. Rev. A* **76** 052509
- [14] Zhou X, Xu X, Chen X and Chen J 2010 *Phys. Rev. A* **81** 012115
- [15] Phoonthong P, Douglas P, Wickenbrock A and Renzoni F 2010 *Phys. Rev. A* **82** 013406
- [16] Arora B and Sahoo B K 2012 *Phys. Rev. A* **86** 033416
- [17] Lundblad N, Schlosser M and Porto J V 2010 *Phys. Rev. A* **81** 031611(R)
- [18] Derevianko A 2010 *Phys. Rev. A* **81** 051606(R)
- [19] Griffin P F, Weatherill K J, MacLeod S G, Potvliege R M and Adams C S 2006 *New J. Phys.* **8** 11
- [20] Arora B and Safronova M S 2010 *Phys. Rev. A* **82** 022509
- [21] Steck D A 2010 Cesium D line data <http://steck.us/alkalidata>
- [22] Kurucz R L and Bell B Atomic line data www.cfa.harvard.edu/amp/ampdata/kurucz23/sekur.html
- [23] Guo S L, Yang J F, Yang B D, Zhang T C and Wang J M 2010 *Proc. SPIE* **7846** 784619
- [24] Brantut J P, Clement J F, Robert de Saint Vincent M, Varoquaux G, Nyman R A, Aspect A, Bourdel T and Bouyer P 2008 *Phys. Rev. A* **78** 031401(R)
- [25] Bernon S, Vanderbruggen T, Kohlhaas R, Bertoldi A, Landragin A and Bouyer P 2011 *New J. Phys.* **13** 065021
- [26] Arnold K J, Baden M P and Barrett M D 2012 *Phys. Rev. Lett.* **109** 153002
- [27] Beugnon J, Jones M P A, Dingjan J, Darquie B, Messin G, Browaeys A and Grangier P 2006 *Nature* **440** 779
- [28] Santori C, Fattal D, Vuckovic J, Salomon G S and Yamamoto Y 2002 *Nature* **419** 594
- [29] Hong C K, Ou Z Y and Mandel L 1987 *Phys. Rev. Lett.* **59** 2044
- [30] Legero T, Wilk T, Hennrich M, Rempe G and Kuhn A 2004 *Phys. Rev. Lett.* **93** 070503
- [31] Knill E, Laflamme R and Milburn G J 2001 *Nature* **409** 46
- [32] Dowling J P, Franson J D, Lee H and Milburn G J 2004 *Quantum Inf. Process.* **3** 205